Process Parameter Optimization in Finish Wire Electrical Discharge Machining of SUS420J2 Steel

Nguyen Trong Mai
Hanoi University of Industry, Hanoi, Vietnam
nguyentrongmai@haui.edu.vn (corresponding author)

Du Thi Kieu Trinh
Hanoi University of Industry, Hanoi, Vietnam
duthikieutrinh@gmail.com

Nguyen Viet Hung
Hanoi University of Industry, Hanoi, Vietnam
nguyenviethung@haui.edu.vn

Received: 8 January 2026 | Revised: 28 January 2026 | Accepted: 8 February 2026

 DOI: https://doi.org/10.48084/etasr.17405

ABSTRACT

Wire Electrical Discharge Machining (WEDM) is a non-traditional manufacturing technique widely used in many industrial sectors. This study aims to identify the optimal settings for three key process parameters in the finishing process of SUS420J2 steel. A 15-trial experimental matrix was established using the Box-Behnken design and incorporating input variables such as peak current, voltage, and pulse-on time. Two output responses were evaluated for each trial: surface roughness and white layer thickness, applying a novel computational framework, Method based on the Removal Effects of Criteria - Rank Order Centroid (MEREC-ROC), to determine the relative importance. The Generalized Reduced Gradient (GRG) algorithm was applied to address the multi-objective optimization challenge, with peak current, voltage, and pulse-on time being measured at 1.94 A, 79.6 V, and 6.96 µs, respectively. Under these conditions, surface roughness and white layer thickness simultaneously reached their minimum levels, at 1.262 µm and 4.828 µm, respectively. Furthermore, this study analyzes in depth the degree to which each process parameter influences the resulting responses.

Keywords-Wire Electrical Discharge Machining (WEDM); SUS420J2 steel; surface roughness; white layer thickness; MEREC-ROC

I. INTRODUCTION

WEDM is a non-contact electro-thermal machining process that plays a crucial role in the precision manufacturing industry, particularly for processing high-hardness materials or ultra-complex components [1, 2]. Unlike conventional subtractive manufacturing methods, WEDM utilizes electrical discharges generated between the electrode and the part within a dielectric medium to cut material, enabling the creation of intricate mold cavities, deep slots, and sharp corners that are inaccessible to mechanical milling cutters [3]. This technology is commonly used in the mold and tooling industry for stamping, casting, and plastic injection molds, in the aerospace industry, in the medical device manufacturing industry, and for mechanical parts requiring micrometer-level dimensional accuracy [4]. WEDM is a process characterized by the interaction of multiple variables, including peak current, voltage, pulse-on time, pulse-off time, electrode characteristics, dielectric fluid properties, and workpiece material properties [5]. Even minor adjustments to a single parameter can lead to significant variations in output responses, including surface roughness, material removal rate, tool wear rate, and surface integrity parameters such as white layer thickness and micro-cracking [6]. Surface roughness and white layer thickness are particularly important because they determine the performance and service life of the product. A rough surface negatively impacts the wear resistance, corrosion protection, and fatigue strength of the manufactured component. Similarly, an extensive white layer thickness tends to concentrate significant stress, easily inducing fatigue cracking, diminishing corrosion resistance, and substantially reducing the long-term durability of the part under dynamic loading conditions, especially for surfaces requiring high precision [7]. Controlling these two parameters is challenging because they are influenced by interrelated and often conflicting technological settings. For example, increasing the peak current and pulse-on time to boost productivity results in higher discharge energy, causing more intense material melting, which leads to increased surface roughness and a thicker white layer containing thermal stress-induced cracks [8]. Conversely, reducing these parameters to achieve a finer surface finish significantly diminishes the machining rate. Additionally, combining different electrode types, such as copper or graphite, with various dielectric fluids alters the heat transfer and ion exchange mechanisms within the discharge gap, leading to a difficult yet significant prediction of surface quality [9]. In multi-objective optimization, determining objective weights is important [10]. Authors in [11] used the entropy method to assign weights to surface finish and Material Removal Rate (MRR) to optimize both simultaneously during the machining of 90CrSi steel. Similarly, the entropy method was applied to weigh surface roughness, MRR, and surface hardness for the multi-objective optimization of AISI H13 steel machining [12]. Grey Relational Analysis (GRA) was used to weigh surface roughness, surface hardness, and MRR when machining medium carbon steel [13]. MEREC has been used to calculate the weights of surface roughness and MRR in order to optimize these parameters concurrently in SKD11 steel machining [14], as well as for surface roughness, tool wear rate, and MRR in EDM processing of 90CrSi steel [15]. Various methodologies have been adopted to determine objective weights in the EDM multi-objective optimization process. However, most published studies rely on objective weighting methods such as entropy, GRA, and MEREC. Using purely objective techniques to determine criteria weights can inadvertently neglect user perspectives on the importance of individual objectives. This oversight may result in a priority ranking that fails to align with user expectations. Conversely, using only subjective methods, such as ROC, Rank Sum (RS), or Rank Reciprocal (RR), to establish weights means that the outcomes will be influenced by personal viewpoints, user experience, or potential bias toward specific criteria [16, 17]. MEREC-ROC is a modern weighting framework that combines the objective MEREC technique with the subjective ROC approach. This hybrid methodology has outperformed individual methods by successfully leveraging the objectivity of MEREC and the subjective ROC perspective of the method [18]. The novelty of the MEREC-ROC method motivated its use in this research to determine objective weights. SUS420J2 steel is a martensitic stainless steel characterized by its high carbon content (approximately 0.15%-0.45%) and its minimum chromium content of 12%. It is known for its exceptional hardness, which is achieved through heat treatment. In the mold industry, it is a premier material for manufacturing precision plastic injection molds, blow molds, glass molds, and mold components that require corrosion resistance from acidic plastics, such as PVC, or that can operate in high-humidity environments. After heat treatment, SUS420J2 typically reaches a hardness of 48–52 HRC, ensuring dimensional stability for complex mold cavities, even during continuous operation at high pressures and temperatures. Based on the aforementioned analysis, this study conducts WEDM experiments on SUS420J2 steel to determine the surface roughness and white layer thickness values. The MEREC-ROC method calculates the weights for these two parameters, and the GRG algorithm solves the multi-objective optimization problem, eliminating the need for additional complex software.

II. MATERIALS AND METHODS

A. *Experimental Setup*

The SUS420J2 steel workpieces used in this experiment were 65 mm long, 20 mm wide, and 8 mm high. The specimens underwent heat treatment to achieve a hardness of 50–52 HRC. This steel grade is equivalent to various international standards, including Z30Cr13 (AFNOR — France), 420S45 (BS — England), X30Cr13 (UNI — Italy), 3Cr13 (GB — China), 2304-03 (SS — Sweden), 30KH13 (GOST — Russia), and X30Cr13 (EN — EU). The primary chemical components of this material are presented in Table I.

TABLE I. MAIN CHEMICAL COMPOSITION OF SUS420J2 STEEL

C	Si	Mn	P	S	Cr
0.32%	0.92%	1.36	0.03%	0.015%	13.2%

The experimental design was formulated based on the Box-Behnken matrix, a widely adopted Design of Experiments (DOE) for statistical optimization studies [19, 20]. Figure 1 shows the components of the experimental system. A CHMER CW 420HS wire-cut machine was used throughout the process. Surface roughness was measured using a Mitutoyo SJ-201 portable surface roughness tester. After machining, the steel specimens were cleaned with alcohol and dried. During the measurement procedure, the stylus traverse direction was adjusted to be perpendicular to the workpiece feed direction. To measure the thickness of the white layer, the samples were sectioned, polished, etched, and examined under a VHX-7000 digital microscope. Three input parameters were chosen for finishing the SUS420J2 steel: peak current, voltage, and pulse-on time. Each factor was assigned three levels corresponding to the coded values -1, 0, and 1, as presented in Table II. These levels were chosen based on the technological capabilities of the experimental equipment and the parameter ranges established in [21, 22]. An experimental matrix was established using the Box-Behnken method, based on the input parameter levels summarized in Table II. This design consists of fifteen trials, including three central point experiments in which all input values correspond to coded level 0, as presented in Figure 2 [19, 20]. The complete experimental matrix is displayed in Table III. In addition to the primary experimental system and design matrix detailed above, the Total Diel MS 7000 dielectric fluid was utilized due to its superior thermal stability and common use in EDM processes. The electrode used throughout the experiments was pure copper (grade C1100), a standard choice for EDM applications.

B. *Utilizing the MEREC-ROC Method to Determine Criteria Weights*

Objective weights were determined using the MEREC-ROC method according to the following procedure [18]:

- Construct a decision-making matrix comprising m alternatives and n criteria, where xij represents the value of criterion j for alternative i.

$$X = \begin{bmatrix} x_{11} & x_{12} & \cdots & x_{1n} \\ x_{21} & x_{22} & \cdots & x_{2n} \\ \cdots & x_{ij} & \cdots & \cdots \\ x_{m1} & x_{m2} & \cdots & x_{mn} \end{bmatrix} \quad (1)$$

(a)

(b)

(c)

(d)

Fig. 1. Experimental system: (a) components, (b) CHMER CW 420HS wire-cut machine, (c) surface roughness tester, (d) VHX 7000 digital microscope.

TABLE II. LEVELS AND VALUES OF INPUT PARAMETERS

Parameter	Code	Symbol	Unit	Value at level		
				-1	0	+1
Peak current	x_1	I	A	1	1.5	2
Voltage	x_2	U	V	70	75	80
Pulse-on time	x_3	T_{on}	µs	5	6	7

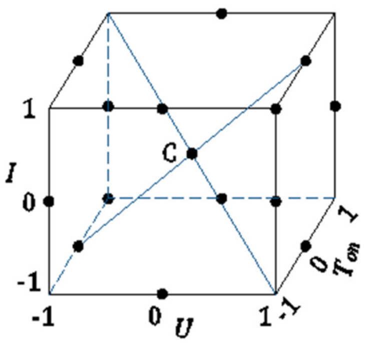

Fig. 2. Box-Behnken design schema for three input parameters.

TABLE III. EXPERIMENTAL DESIGN MATRIX

No.	Code value			Real value			Response	
	x_1	x_2	x_3	I (A)	U (V)	T_{on} (µs)	R_a (µm)	H_{WL} (µm)
1	-1	0	1	1	75	7	1.578	12.62
2	0	1	-1	1.5	80	5	1.521	17.75
3	0	-1	1	1.5	70	7	1.438	20.89
4	-1	0	-1	1	75	5	1.483	17.31
5	0	0	0	1.5	75	6	1.446	14.73
6	1	-1	0	2	70	6	1.642	18.14
7	1	0	-1	2	75	5	1.731	20.66
8	0	-1	-1	1.5	70	5	1.159	17.72
9	0	0	0	1.5	75	6	1.651	17.39
10	1	1	0	2	80	6	1.497	12.37
11	-1	1	0	1	80	6	1.394	21.67
12	1	0	1	2	75	7	1.128	10.37
13	-1	-1	0	1	70	6	1.444	20.02
14	0	0	0	1.5	75	6	1.557	10.8
15	0	1	1	1.5	80	7	1.483	7.29

- Calculate the normalized values for the "larger-is-better" and "smaller-is-better" criteria, respectively:

$$n_{ij} = \frac{min x_{ij}}{x_{ij}} \quad (2)$$

$$n_{ij} = \frac{x_{ij}}{max\ x_{ij}} \quad (3)$$

- Compute the overall performance of the alternatives:

$$S_i = Ln\left[1 + \left(\frac{1}{n}\sum_j^n \left|ln(n_{ij})\right|\right)\right] \quad (4)$$

- Determine the performance of the modified alternatives:

$$S'_{ij} = Ln\left[1 + \left(\frac{1}{n}\sum_{k,k\neq j}^n \left|ln(n_{ij})\right|\right)\right] \quad (5)$$

- Calculate the absolute deviation values:

$$E_j = \sum_i^m \left|S'_{ij} - S_i\right| \quad (6)$$

- Compute the MEREC weights for the criteria:

$$w_j = \frac{E_j}{\sum_j^n E_j} \quad (7)$$

- Rank the criteria in order of descending priority, with the most significant criterion ranked as 1 and the least significant criterion ranked as n.
- Calculate the final weights for the criteria:

$$w_j = \frac{1}{n}\sum_{h=i}^{n}\frac{1}{h} \quad (8)$$

where h is the rank of criterion j.

III. RESULTS AND DISCUSSION

The experiments were conducted in the order specified in Table II. Each trial was repeated three times using three separate steel specimens. For these trials, R_a and H_{wl} were measured at least three times on each sample. The values recorded in Table II represent the average of these consecutive measurements. The surface roughness values from all experiments corresponded to grade 7 roughness, aligning with the experimental data reported in [23]. Figures 3 and 4, respectively, present the individual effects of the input parameters on surface roughness and the interactive effects of each pair of input variables on the same response.

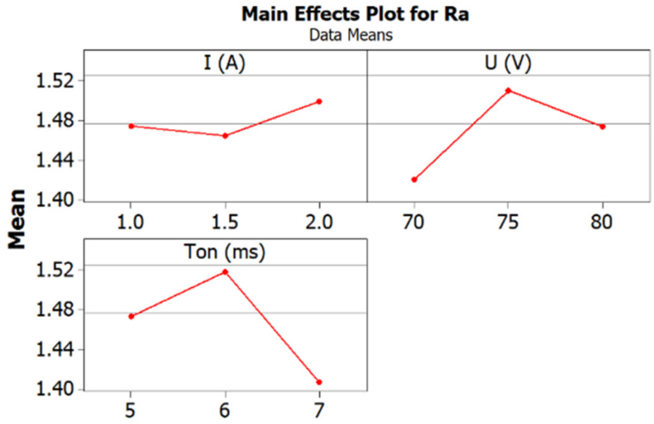

Fig. 3. Effects of process parameters on R_a.

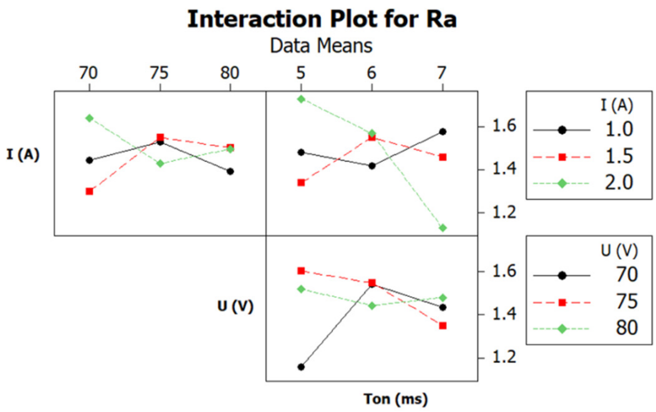

Fig. 4. Interactive effects of process parameters on R_a.

As shown in Figure 3, as the peak current increases from 1 A to 1.5 A, surface roughness decreases slowly. However, further increasing the current leads to an increase in surface roughness. Increasing the voltage from 70 V to 75 V causes a rapid increase in surface roughness. However, subsequently increasing the voltage leads to a sharp decline in Ra. Similarly, increasing the pulse-on time from 5 ms to 6 ms results in a swift rise in surface roughness, followed by a rapid decrease as the pulse-on time continues to increase [24, 25]. The diagrams in Figure 4 further demonstrate the complexity of the ways the input parameters influence surface roughness. For example, examining the interaction between peak current and pulse-on time reveals that, at a current of 1 A, increasing the pulse-on time from 5 ms to 6 ms reduces surface roughness. However, increasing it from 6 ms to 7 ms causes roughness to rise. Conversely, at 1.5 A, increasing the pulse-on time from 5 ms to 6 ms leads to higher roughness; however, a further increase results in a decrease. For 2 A, surface roughness decreases moderately when pulse-on time increases from 5 ms to 6 ms, but drops significantly when it increases from 6 ms to 7 ms [24, 25]. Figures 5 and 6 show the complexity of the magnitude and patterns of influence of the input parameters on white layer thickness. Increasing the peak current from 1 A to 1.5 A reduces the white layer thickness. Further increases in current leave the thickness virtually unchanged. Similarly, increasing the voltage from 70 V to 75 V causes a rapid decrease in Hwl; however, further increments result in negligible changes. Regarding pulse-on time, increasing it from 5 ms to 6 ms leads to a moderate reduction in white layer thickness. However, increasing it from 6 ms to 7 ms triggers a rapid decline [24, 25].

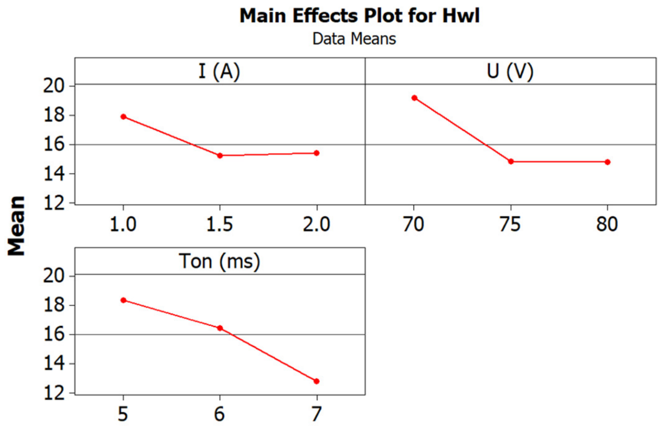

Fig. 5. Effects of process parameters on H_{wl}.

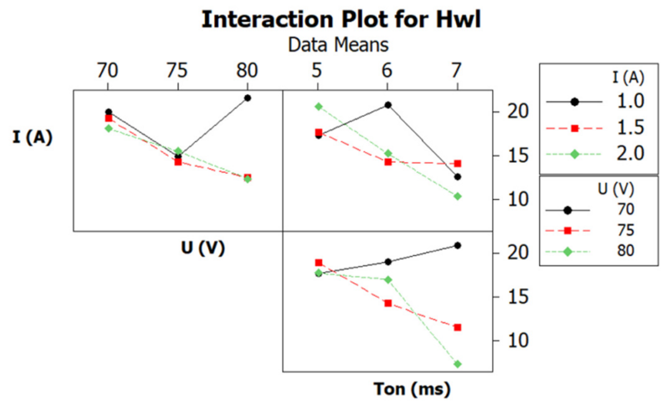

Fig. 6. Interactive effects of process parameters on H_{wl}.

Figure 6 provides deeper insights into the interactive influences on white layer thickness. Regarding the interaction between peak current and voltage, increasing the voltage consistently reduces H_{wl} at 1.5 A and 2 A. However, at a current of 1 A, the behavior differs. White layer thickness decreases rapidly as the voltage rises from 70 V to 75 V. Then, it increases sharply as the voltage continues to rise. The aforementioned analyses of the effects of input parameters on surface roughness and white layer thickness highlight the difficulty of controlling these variables to minimize both output responses simultaneously. Consequently, a multi-objective optimization approach is necessary. Based on the data in Table III, two regression equations were developed to represent the relationship between the responses and the input parameters [26]:

$$R_a = 1.5513 + 0.0123 \times x_1 + 0.0265 \times x_2 - 0.0333 \times x_3 + 0.0113 \times x_1^2 - 0.0684 \times x_2^2 - 0.0826 \times x_3^2 - 0.0237 \times x_1 \times x_2 - 0.1745 \times x_1 \times x_3 - 0.0792 \times x_2 \times x_3 \quad (9)$$

$$H_{wl} = 14.3067 - 1.2600 \times x_1 - 2.2113 \times x_2 - 2.7838 \times x_3 + 1.5354 \times x_1^2 + 2.2079 \times x_2^2 - 0.6021 \times x_3^2 - 1.8550 \times x_1 \times x_2 - 1.4000 \times x_1 \times x_3 - 3.4075 \times x_2 \times x_3 \quad (10)$$

The optimization problem is now formulated as:

$$\begin{cases} f(x) = w_1 \times R_a + w_2 \times H_{wl} \rightarrow \min \\ -1 \leq x_1, x_2, x_3 \leq 1 \\ R_a, H_{wl} > 0 \end{cases} \quad (11)$$

where w_1 and w_2 represent the weights of R_a and H_{wl}, respectively. The MEREC weights for surface roughness and white layer thickness were calculated as 0.3225 and 0.6775, respectively, by applying (1) to (7). Thus, white layer thickness is ranked first and surface roughness second in terms of priority. Applying (8) subsequently provided the final MEREC-ROC weights of 0.25 for R_a and 0.75 for H_{wl}. These values were used to solve the multi-objective optimization problem described by (11). Using the Excel Solver tool and the GRG algorithm, the optimization identified the optimal values for x_1, x_2, and x_3 as 0.88, 0.92, and 0.96, respectively. These correspond to optimal physical values of 1.94 A for peak current, 79.6 V for voltage, and 6.96 ms for pulse-on time. According to the model's predictions, the surface roughness and white layer thickness at these optimal settings are 1.139 µm and 4.53 µm, respectively. These values were used to conduct confirmation experiments with three samples, the results of which are summarized in Table IV. In this context, $R_a^{(op)}$ and $H_{wl}^{(op)}$ represent the R_a and H_{wl} values obtained by solving the optimization problem, and $R_a^{(me)}$ and $H_{wl}^{(me)}$ correspond to the experimental R_a and H_{wl} values, respectively.

TABLE IV. EXPERIMENTAL RESULTS USING OPTIMAL PROCESS PARAMETER VALUES

Exp.	$R_a^{(op)}$ (µm)	$R_a^{(me)}$ (µm)	$H_{wl}^{(op)}$ (µm)	$H_{wl}^{(me)}$ (µm)
1	1.139	1.231	4.530	4.778
2	1.139	1.218	4.530	4.916
3	1.139	1.337	4.530	4.790
Average	1.139	1.262	4.530	4.828

The values for surface roughness and white layer thickness were 1.262 µm and 4.828 µm, respectively. Thus, the deviation between the calculated and experimental values is only 9.75% for surface roughness and 6.17% for white layer thickness, validating the accuracy of the experimental design, optimization procedures, and precision of the validation trials.

IV. CONCLUSIONS

Surface roughness and white layer thickness significantly impact the operational performance and service life of mechanical products. This study conducted experiments to determine the optimal values of the following process parameters: peak current, voltage, and pulse-on time. The goal was to minimize both output responses during the Wire Electrical Discharge Machining (WEDM) of SUS420 steel. For the first time, the Method based on the Removal Effects of Criteria - Rank Order Centroid (MEREC-ROC) was used to calculate objective weights for a multi-objective optimization problem:

- The weights for surface roughness and white layer thickness were determined to be 0.25 and 0.75, respectively.
- The optimal configuration for peak current, voltage, and pulse-on time was identified as 1.94 A, 79.6 V, and 6.96 ms, respectively. With this optimal parameter set, surface roughness was 1.262 µm, and white layer thickness was 4.828 µm.

Future research should focus on optimizing the machining process for this steel grade by considering responses such as the tool wear rate, the material removal rate, and the surface microstructure. Additionally, investigating other WEDM process parameters, such as electrode types, pulse-off time, and dielectric fluid characteristics, is essential to fully optimize the machining of this material.

REFERENCES

[1] K. Ukey, A. R. Sahu, S. S. Gajghate, A. K. Behera, C. Limbadri, and H. Majumder, "Wire electrical discharge machining (WEDM): Review on current optimization research trends," *Materials Today: Proceedings*, 2023. https://doi.org/10.1016/j.matpr.2023.06.113.

[2] S. S. Sidhu and M. Yazdan, "Comparative analysis of MCDM techniques for EDM of SiC/A359 composite," *Arabian Journal for Science and Engineering*, vol. 43, pp. 1093–1102, 2018, https://doi.org/10.1007/s13369-017-2726-5.

[3] Y. Yildiz, "Application of multi-criteria decision making (MCDM) methods on a meso-scale electrical discharge drilling (EDD) process," *SN Applied Sciences*, vol. 2, 2020, Art. no. 1872, https://doi.org/10.1007/s42452-020-03668-0.

[4] N. V. Thien and N. H. Son, "Material selection for PMEDM process," *International Journal of Mechanical Engineering and Robotics Research*, vol. 13, no. 3, pp. 315–324, 2024, https://doi.org/10.18178/ijmerr.13.3.315-324.

[5] J. D. Patel and K. Maniya, "A review on wire cut electrical discharge machining process for metal matrix composite," *Procedia Manufacturing*, vol. 20, pp. 253–258, 2018, https://doi.org/10.1016/j.promfg.2018.02.037.

[6] M. A. C. Abdullah, A. Yahya, and W. N. W. M. Shukri, "Integrated control of electrical discharge machining using PSoC," *Journal of Physics: Conference Series*, vol. 1529, 2020, Art. no. 042087, https://doi.org/10.1088/1742-6596/1529/4/042087.

[7] R. Świercz, D. Oniszczuk-Świercz, and L. Dąbrowski, "Electrical discharge machining of difficult-to-cut materials," *Archives of Mechanical Engineering*, vol. 65, no. 4, pp. 461–477, 2018, https://doi.org/10.24425/ame.2018.125437.

[8] Y. Shireesha, A. Rahul, B. Jayasurya, and P. Pavan Kumar, "Study and calibration of electrical discharge machining (EDM)," *International Journal of Research Publication and Reviews*, vol. 5, pp. 5209–5228, 2024.

[9] C.-H. Lee and T.-S. Lai, "An intelligent system for improving electric discharge machining efficiency using artificial neural network and adaptive control of debris removal operations," *IEEE Access*, vol. 9, pp. 75302–75312, 2021, https://doi.org/10.1109/ACCESS.2021.3080297.

[10] D. D. Trung, "A combination method for multi-criteria decision-making problem in turning process," *Manufacturing Review*, vol. 8, 2021, Art. no. 26, https://doi.org/10.1051/mfreview/2021024.

[11] T. Q. Huy, T. H. Danh, B. T. Danh, N. V. Cuong, N. M. Cuong, and N. T. Tu, "Multi-criteria decision making in wire-EDM process using MARCOS method," in *Lecture Notes in Networks and Systems*, vol. 602, pp. 699–706, 2023, https://doi.org/10.1007/978-3-031-22200-9_74.

[12] G. K. Bose and K. K. Mahapatra, "Multi-criteria decision making of machining parameters for die-sinking EDM process," *International Journal of Industrial Engineering Computations*, vol. 6, pp. 241–252, 2015, https://doi.org/10.5267/j.ijiec.2014.10.005.

[13] N. D. Luan, N. D. Minh, and L. T. P. Thanh, "Multi-criteria decision making in machining process," *International Journal of Trend in Scientific Research and Development*, vol. 3, pp. 112–115, 2019.

[14] T. H. Danh, T. Q. Huy, P. D. Lam, N. M. Cuong, H. X. Tu, and V. N. Pi, "A study on multi-criteria decision-making in powder-mixed electric discharge machining cylindrical shaped parts," *EUREKA: Physics and Engineering*, vol. 2022, pp. 123–129, 2022, https://doi.org/10.21303/2461-4262.2022.002367.

[15] T. P. T. Le, V. T. Dinh, T. Q. D. Nguyen, D. B. Vu, and T. T. Vu, "Application of the multi-criteria decision method to find the best input factors for electrical discharge machining 90CrSi tool steel using graphite electrodes," *Engineering, Technology and Applied Science Research*, vol. 14, no. 6, pp. 18883–18888, 2024, https://doi.org/10.48084/etasr.9114.

[16] R. Kumar, S. Singh, P. S. Bilga, J. Singh, S. Singh, M.-L. Scutaru, and C. I. Pruncu, "Revealing the benefits of entropy weights method for multi-objective optimization in machining operations: A critical review," *Journal of Materials Research and Technology*, vol. 10, pp. 1471–1492, 2021, https://doi.org/10.1016/j.jmrt.2020.12.114.

[17] I. Z. Mukhametzyanov, "Specific character of objective methods for determining weights of criteria in MCDM problems: Entropy, CRITIC, SD," *Decision Making: Applications in Management and Engineering*, vol. 4, no. 2, pp. 76–105, 2021, https://doi.org/10.31181/dmame210402076i.

[18] B. T. T. Trang, D. D. Trung, and R. Turmanidze, "A novel approach for criteria weighting to enhance ranking stability of alternatives for industrial equipment and material selection," *Advanced Engineering Letters*, vol. 4, no. 3, pp. 118–133, 2025, https://doi.org/10.46793/adeletters.2025.4.3.2.

[19] D. D. Trung, "Influence of cutting parameters on surface roughness during milling AISI 1045 steel," *Tribology in Industry*, vol. 42, no. 4, pp. 658–665, 2020, https://doi.org/10.24874/ti.969.09.20.11.

[20] A. R. A. Aziz and S. A. Aziz, "Application of Box–Behnken design to optimize the parameters for kenaf–epoxy as noise absorber," *IOP Conference Series: Materials Science and Engineering*, vol. 454, 2018, Art. no. 012001, https://doi.org/10.1088/1757-899X/454/1/012001.

[21] N. L. S. Hashim *et al.*, "Review on an electrical discharge machining servomechanism system," *Scientia Iranica, Transaction B: Mechanical Engineering*, vol. 22, no. 5, pp. 1813–1832, Oct. 2015.

[22] X. Zhu, G. Li, J. Mo, and S. Ding, "Multi-channel electrical discharge machining of titanium alloy Ti-6Al-4V with semiconductor electrodes," *Journal of Physics: Conference Series*, vol. 2612, 2023, Art. no. 012011, https://doi.org/10.1088/1742-6596/2612/1/012011.

[23] H. Anwar, S. K. Shather, and W. S. Khudhir, "WEDM process parameters analysis and optimization: A review," *Ciencia y Tecnología – Serie de Conferencias*, vol. 3, 2024, https://doi.org/10.56294/sctconf2024860.

[24] S. H. Aghdeab, V. N. Najm, and A. M. Saleh, "Surface roughness evaluation in WEDM using Taguchi parameter design method," *Engineering and Technology Journal*, vol. 36, no. 1A, pp. 60–64, 2018, https://doi.org/10.30684/etj.36.1A.9.

[25] M. Yuvaraj, "Study the various parameters of wire cut electrical discharge machining," *International Journal of Research Publication and Reviews*, vol. 5, no. 1, pp. 235–242, 2024.

[26] D. D. Trung, "Influence of cutting parameters on surface roughness in grinding of 65G steel," *Tribology in Industry*, vol. 43, no. 1, pp. 167–176, 2021, https://doi.org/10.24874/ti.1009.11.20.01.